HAL
open science

Localization and chemical forms of cadmium in plant samples by combining analytical electron microscopy and X-ray spectromicroscopy

M.-P. Isaure, Barbara Fayard, Géraldine Sarret, Sébastien Pairis, Jacques Bourguignon

To cite this version:

M.-P. Isaure, Barbara Fayard, Géraldine Sarret, Sébastien Pairis, Jacques Bourguignon. Localization and chemical forms of cadmium in plant samples by combining analytical electron microscopy and X-ray spectromicroscopy. Spectrochimica Acta Part B: Atomic Spectroscopy, 2006, 61 (12), pp.1242-1252. 10.1016/j.sab.2006.10.009 . hal-00126972

HAL Id: hal-00126972

https://hal.science/hal-00126972

Submitted on 7 Jan 2008

HAL is a multi-disciplinary open access archive for the deposit and dissemination of scientific research documents, whether they are published or not. The documents may come from teaching and research institutions in France or abroad, or from public or private research centers.

L'archive ouverte pluridisciplinaire **HAL**, est destinée au dépôt et à la diffusion de documents scientifiques de niveau recherche, publiés ou non, émanant des établissements d'enseignement et de recherche français ou étrangers, des laboratoires publics ou privés.

Localization and chemical forms of cadmium in plant samples by combining analytical electron microscopy and X-ray spectromicroscopy

Marie-Pierre Isaure [a,b,], Barbara Fayard [c,d], Géraldine Sarret [b], Sébastien Pairis [e], and Jacques Bourguignon [f]*

a- Section d'Application des Traceurs, LITEN, CEA-Grenoble, 17, rue des Martyrs, 38054 Grenoble cedex 9, France

b- Environmental Geochemistry Group, LGIT, UMR 5559, Université J. Fourier and CNRS, BP 53, 38041 Grenoble cedex 9, France

c- Laboratoire de Physique des Solides, UMR 8502 Université Paris Sud, 91405 Orsay, France

d- European Synchrotron Radiation Facility, ID-21, BP220, 38043 Grenoble, France

e- Laboratoire de Cristallographie, UPR 5031, 25 Avenue des Martyrs, BP 166, 38042 Grenoble cedex 9 France

f- Laboratoire de Physiologie Cellulaire Végétale, UMR 5168 CEA/CNRS/INRA/UJF, DRDC, CEA-Grenoble, 17 Avenue des Martyrs, 38054 Grenoble cedex 9, France

* Corresponding author: Marie-Pierre Isaure, Environmental Geochemistry Group, LGIT, Phone: 33 4 76 82 80 21, Fax: 33 4 76 82 81 01, Email: mpisaure@ujf-grenoble.fr

Abstract

Cadmium (Cd) is a metal of high toxicity for plants. Resolving its distribution and speciation in plants is essential for understanding the mechanisms involved in Cd tolerance, trafficking and accumulation. The model plant *Arabidopsis thaliana* was exposed to cadmium under controlled conditions. Elemental distributions in the roots and in the leaves were determined using scanning electron microscopy coupled with energy dispersive X-ray microanalysis (SEM-EDX), and synchrotron-based micro X-ray fluorescence (µ-XRF), which offers a better sensitivity. The chemical form(s) of cadmium was investigated using Cd L_{III}-edge (3538 eV) micro X-ray absorption near edge structure (µ-XANES) spectroscopy. Plant µ-XANES spectra were fitted by linear combination of Cd reference spectra. Biological sample preparation and conditioning is a critical point because of possible artifacts. In this work we compared freeze-dried samples analyzed at ambient temperature and frozen hydrated samples analyzed at -170°C. Our results suggest that in the roots Cd is localized in vascular bundles, and coordinated to S ligands. In the leaves, trichomes (epidermal hairs) represent the main compartment of Cd accumulation. In these specialized cells, µ-XANES results show that the majority of Cd is bound to O/N ligands likely provided by the cell wall, and a minor fraction could be bound to S-containing ligands. No significant difference in Cd speciation was observed between freeze-dried and frozen hydrated samples. This work illustrates the interest and the sensitivity of Cd L_{III}-edge XANES spectroscopy, which is applied here for the first time to plant samples. Combining µ-XRF and Cd L_{III}-edge µ-XANES spectroscopy offers promising tools to study Cd storage and trafficking mechanisms in plants and other biological samples.

Keywords : cadmium; plant; SEM-EDX; micro-XRF; micro-XANES

1. Introduction

Contamination of the earth surface with cadmium has increased during the last century due to mining, atmospheric deposition from smelters, and application of sewage sludge and phosphate fertilizers [1]. Cadmium is one of the most toxic heavy metal for plants. One of the strategies for plants to resist the toxicity of Cd is the complexation with strong ligands such as thiol groups provided by cysteine, an amino-acid constituting peptides often mentioned in Cd resistance, namely glutathione, phytochelatins and metallothioneins [2]. Another mechanism involved in the resistance to toxic metals is the compartmentalization in specific tissues or cellular compartments. For instance, in leaves of the hyperaccumulating plant *Thlaspi caerulescens*, the epidermis is the Cd richest tissue [3]. However, Ma et al. [4] stated that the mesophyll constitutes the major storage site due to its higher biomass. In roots, Cd might be stored in the apoplasm particularly in cell walls [3,5]. Wojcik et al. [3] also reported a localization in cortex parenchyma cells, endodermis, parenchyma cells of the central cylinder and xylem vessels. In the hyperaccumulator *Arabidopsis halleri*, a high Cd content was found in the trichomes (non glandular unicellular epidermal hairs) of the leaves, but the mesophyll was the main accumulating compartment [6]. Trichomes of Indian mustard [7] and tobacco [8] were also found to accumulate cadmium, suggesting a possible role of these epidermal structures in the detoxification process.

Although *Arabidopsis thaliana* is not a metal hyperaccumulating species, processes controlling metal homeostasis in this plant are actively studied [9,10 and references therein]. Indeed, its genome is close to the one of the hyperaccumulator *Arabidopsis halleri*, so the comparison between the two species is appropriate. Moreover, the genes involved in metal

tolerance and accumulation that have been identified in *A. halleri* are present in *A. thaliana*, but regulated differently [11 and references therein]. The study of Cd localization and speciation in *A. halleri* is in progress, and will be the subject of a future publication.

A study on the distribution of Cd in *A. thaliana* reported high concentrations of the metal in trichomes [12]. Although the role of glutathione has been reported for metal detoxification in these specialized epidermal cells [13,14], the possible binding of Cd to this peptide remains elusive. Likewise, the chemical form(s) of Cd in the other *A. thaliana* tissues remain(s) unknown.

The aim of this study was to determine the distribution of Cd in the different tissues (leaves and roots) of *A. thaliana*, and also to determine the chemical form(s) of accumulated Cd in these tissues. The distribution of Cd in the roots and in the leaves was investigated using scanning electron microscopy coupled with energy dispersive X-ray analysis (SEM-EDX) and synchrotron-based micro X-ray fluorescence (µ-XRF), which are complementary techniques in terms of sensitivity and lateral resolution. The chemical form of the metal was then established by micro X-ray absorption near edge structure (µ-XANES) at the Cd L_{III}-edge on the different tissues. Although µ-XANES have been largely applied to investigate metal speciation in soils and sediments [15], it was less applied to biological samples. µ-XANES has been previously used in plant samples to evidence the local chemistry of thallium (L_{III}-edge) in the plant *Iberis intermedia* [16], of selenium (K-edge) in *Arabidopsis thaliana* [17] and in Astragalus plants [18], of nickel and manganese (K-edge) in annual rings of *Salix nigra* [19], and of chromium (K-edge) in subterranean clover [20], with a lateral resolution higher than 5 µm x 5 µm. It has been also applied to characterize interactions between metal(loïd)s and bacteria, for instance, chromium (K-edge) in cells of *Pseudomonas fluorescens* using a lateral resolution lower

than 1 µm [21], and selenium (K-edge) in *Pseudomonas syringae* with a beam diameter higher than 1 µm [22]. To our knowledge, it has never been used to investigate Cd at the L_{III}-edge in plant samples. Artifacts resulting from the preparation and irradiation of biological samples have been observed [23], and in this study, we compared freeze-dried plant samples analyzed at ambient temperature and frozen hydrated samples analyzed at -170°C using a cryostat.

2. Experimental

2.1. Plant Culture and Cadmium Contents

Seeds of *Arabidopsis thaliana* wild type (variety Columbia) were germinated and grown in a controlled growth chamber, in Petri dishes containing sucrose and agar-enriched nutritive medium. Twelve days after germination, 40 seedlings were transferred in Petri dishes containing the same medium contaminated or not (control) with 200 µM $Cd(NO_3)_2$. After 4 days of treatment, root length was measured with a ruler (precision: 1 mm) on 20 plants for each treatment, and expressed as mean (cm) ± standard deviation (SD). Plants were harvested and rinsed with deionised water. Leaves and roots were separated, frozen in liquid nitrogen, and some of them were freeze-dried at –36°C.

For chemical analysis, freeze-dried roots and leaves were ground and digested in HNO_3/ HCl (3/1, v/v) at 85°C. Cd concentrations were determined using inductively coupled plasma mass spectrometry (ICP-MS).

2.2. Cadmium Model Compounds

Various organic and mineral Cd model compounds were synthesized for comparison with plant samples (fingerprint approach). Optimal experimental conditions

(pH, concentrations) were calculated using PHREEQC-2 code [24] to ensure the presence of the required Cd-complex and to avoid precipitation. Cd^{2+}, Cd-malate, Cd-citrate, Cd-gluthatione, Cd-histidine, and Cd-cysteine complexes were prepared as aqueous solutions as follows. Solution containing 50 mM $Cd(NO_3)_2$ at pH = 3.0 was used as model for the aqueous complex. Cd-malate and Cd-citrate were prepared at a Cd concentration of 25 mM and a metal/ligand (M/L) ratio of 1/10, and at a pH of 5.1. Cd-glutathione and Cd-histidine were prepared with the same M/L ratio and 12.5 mM Cd at pH of 2.7 and 6.7, respectively. Cd cysteine containing 12.5 mM Cd was prepared at a M/L ratio of 5 at pH 2.8.

Cd-pectin, Cd-cellulose, and Cd-cell wall extracted from tobacco roots were prepared as solid compounds. Cd-pectin complexes were prepared by introducing pectin extracted from apples esterified at 70 to 75% (Fluka) in 0.19 mM Cd and 0.04 mM $Cd(NO_3)_2$ in a ratio M/L = 1/130, and 1/650 respectively, and stirring the gel for 3 hours at fixed pH 5.0 by addition of NaOH or HNO_3. Since the Cd-pectin complexes could not be separated by centrifugation, the gel was directly freeze-dried at -50°C. Cd-cellulose complexes were prepared with the same M/L ratios and with Cd concentrations of 15 and 75 µM using the same procedure, except that the suspension was centrifuged, and the pellets were frozen and freeze-dried at -50°C. Cell walls were obtained by immersing fresh roots of 4-week old tobacco plants in a 1% v/v Triton X100 detergent solution with 1 mM $CaCl_2$ for 28 days to remove the cell content. The detergent was then removed by washing with a 1 mM $CaCl_2$ solution. The entire treatment was carried out at 4°C. Cd adsorbed on cell walls was then prepared by adding 8.89 mM (1000 $mg.kg^{-1}$) $Cd(NO_3)_2$ to a suspension of cell walls, centrifugating the suspension after 3 days of contact (final pH = 5.9), and freeze-drying the pellet. The final Cd concentration in cell walls was 2000

mg.kg^{-1} DW. Pellets were frozen and freeze-dried at -50°C.

Solid-state Cd reference compounds were prepared as follows. Cd phosphate ($Cd_5H_2(PO_4)_4.4H_2O$) was synthesized by adding 50 mM $Cd(NO_3)_2$ to 50 mM NaH_2PO_4 (3/2, v/v) at pH 5.5. Cd oxalate (CdC_2O_4) was precipitated by adding 1 mM $Cd(NO_3)_2$ to 1 mM $Na_2C_2O_4$ (1/1, v/v) at pH 7.1. After precipitation, Cd phosphate and Cd oxalate were centrifugated, rinsed in deionized water, filtered at 0.45 µm, dried at 40°C, and prepared as pressed pellets. Commercial CdS, $CdSO_4$, $CdCl_2$, $CdCO_3$, CdO, and Cd acetate powders were used as standard references.

2.3. Scanning Electron Microscopy Coupled with Energy-Dispersive X-Ray Microanalysis (SEM-EDX)

Six freeze-dried samples were mounted on carbon stubs using carbon tape, and coated with carbon. They were imaged and analyzed using a scanning electron microscope (Jeol-JSM 840A) equipped with an EDX system (Kevex Si(Li) diode), with a chamber pressure of 10^{-6}-10^{-5} Torr, and an accelerating voltage of 10 kV. X-ray fluorescence maps, profiles of concentrations along transect lines and X-ray fluorescence spectra were recorded on chosen spots. For semi-quantification, spectra were analyzed by applying ZAF calculation (IDFix software).

2.4. Micro X-ray Fluorescence (µ-XRF) and X-ray Absorption Near Edge Structure (µ-XANES) Spectroscopy

µ-XRF and Cd L_{III}-edge µ-XANES analyses were conducted on the ID-21 spectromicroscopy beamline at the European Synchrotron Radiation Facility (ESRF, Grenoble, France). The X-ray photons were focused by a Fresnel zone plate providing a

sub-micron resolution [25]. The X-ray beam was monochromatized using a fixed exit Si(111) two-crystal monochromator. All measurements were performed under vacuum (10^{-7}-10^{-8} Torr).

The same samples were recorded in freeze-dried state at room temperature and in frozen hydrated state at -170°C using a N_2 cryostat. Six *Arabidopsis thaliana* leaves and five roots taken from distinct plantlets were sandwiched between 4 µm-thick Ultralene® films. Elemental maps were obtained by scanning the samples with a beam size on the sample of 0.9 µm (H) x 0.3 µm (V) FWHM, while recording the X-ray fluorescence spectrum with a one-element solid-state High Purity Germanium detector. Because plants contain a large amount of potassium, the K_α fluorescence emission line (3314 eV) overlaps the most intense Cd line, Cd $L_{\alpha 1}$ (3133 eV). Consequently, phosphorus, sulfur, chloride, and cadmium maps were recorded using an incident energy below the absorption edge of potassium (3550 eV), while potassium and calcium maps were recorded at 4100 eV. For µ-XRF maps, the fluorescence yield was normalized by the incident photon intensity (I_0) measured with a photodiode made of a 0.75 µm thick aluminum foil. About six areas of leaves presenting trichomes and veins, and five portions of roots were mapped either on freeze-dried or frozen samples. Some X-ray fluorescence spectra were recorded at 3550 eV on points of interest evidenced by the maps.

Cd L_{III}-edge XANES spectra were collected in fluorescence mode with the Ge detector or in transmission mode using a photodiode depending on Cd concentration, in the energy range 3530-3580 eV. Solution references were recorded at –170°C and contained 25% (v/v) glycerol to minimize the formation of ice crystals. Solid references were diluted in boron nitride, pressed as pellets, and recorded at ambient temperature. For

Cd-pectin and Cd-cellulose, both freeze-dried and frozen hydrated states were analyzed. For plant samples, µ-XANES spectra were recorded on points of interest evidenced by µ-XRF mapping, at -170°C and at ambient temperature. Plant spectra were not recorded above 3560 eV because of the K-edge of potassium arising at 3561 eV.

XANES data were analyzed using WinXAS. The collected scans were calibrated using a Cd metal foil (the energy origin E_0, which theoretical value is 3538 eV, was taken at the inflection point of the absorption edge), averaged, background subtracted and normalized using a linear or a two-degree polynomial. Theoretical simulations of XANES data provide information on the electronic structure of the target atom. However, this approach is unadapted to biological or environmental systems generally containing a distribution of disordered species. Therefore, we used a fingerprint approach where the unknown spectra were compared to a library of reference compound spectra, and simulated by linear combinations. The quality of the fits was quantified by the normalized sum-squares residuals $NSS = \Sigma(\text{Xanes}_{\text{experimental}} - \text{Xanes}_{\text{fit}})^2 / \Sigma(\text{Xanes}_{\text{experimental}})^2 \times 100$, in the 3530-3580 eV range.

3. Results

3.1. Plant Growth and Cadmium Contents

Figure 1 shows that the root growth, estimated by the root length, was strongly inhibited under Cd exposure. Root length was 4.4 cm ± 0.7 cm (SD) before the transfer on contaminated medium, and 4.5 ± 0.6 cm after 4 days of exposition to Cd compared to 6.8 ± 1.2 cm for the control. The number of lateral roots was also reduced in the Cd-containing medium. The number of leaves was similar in the Cd medium compared to the control, but leaves were smaller in the former medium. A slight chlorosis (yellowish

colour) corresponding to chlorophyll dysfunction was observed in the contaminated medium, indicating that the plants suffered from pronounced but non lethal Cd toxicity. Numerous trichomes were observed on the surface of the leaves (Figure 1D), and no difference was observed between the control and the Cd-exposed plants concerning the number and morphology of the trichomes. After four days of treatment, Cd concentration amounted to 550 $mg.kg^{-1}$ dry weight in leaves, and 2530 $mg.kg^{-1}$ dry weight in roots.

3.2. Elemental Distribution by SEM-EDX and µ-XRF

SEM-EDX images of freeze-dried leaves show that the integrity of the trichomes was preserved (Figure 2A). Backscattering electron images evidence an enrichment of heavy elements in a strip located at the half eight of the trunk of the trichome, and in the tip of the branches (Figure 2B). EDX profiles collected on the trunk clearly show an enrichment in Cd, P, and Mn in the strip, along with a decrease in Mg, S, Cl, K and Ca content (Figure 2C-F). Trichome tips can also contain large amounts of Cd, Cl, Mn and Si. Small bumps (~ 2 µm in diameter) present at the surface of the trichomes, which are micro-ornamentations arising from the cell wall or cuticle, are enriched with Cd, Mn, P, and Ca (Figure 3).

Micro X-ray fluorescence maps confirm that in leaves, Cd is mostly located in the trichomes with the highest amounts of metal encountered in the strip of the trunk, in the end of the branches, and in the small bumps of the trichome surface (Figure 4A). The metal is even more concentrated in the outer parts of this strip, suggesting that it is associated to the cell wall or cuticle. Several maps collected on leaves of other *A. thaliana* plants showed a similar distribution. The X-ray fluorescence spectrum collected on the leaf tissue in point 2 exhibits a weak Cd signal (Figure 4D). Considering the high

sensitivity of µ-XRF for trace elements (sub mg kg^{-1}, [26]), this indicates a very low Cd concentration in the leaf tissue. At the opposite, the Cd signal recorded on the trichome strip in point 1 is about two order of magnitude higher (Figure 4C). The leaves studied being densely covered by trichomes (Figure 1D), this suggests that trichomes are the major compartment of Cd accumulation in the leaves. Trichomes are also enriched with Ca while P, S, Cl and K are more concentrated in the leaf tissue than in the trichomes. Cadmium is possibly co-located with phosphorus in the strip and in the bumps of the trichomes. X-ray fluorescence maps collected on frozen samples showed similar distribution of the chemical elements (not shown).

Several roots were examined by µ-XRF, and elemental distributions for a representative root are presented in Figure 4B. Cd is mainly distributed in the central vascular bundles, where it is co-located with S and Ca. The X-ray fluorescence spectrum collected in the Cd-enriched vascular bundle (Figure 4E) confirms the occurrence of S and Cd, whose concentrations decrease near the surface of the root (Figure 4F). Note that phosphorus and cadmium distributions differ in the root, P being essentially localized in the central cylinder.

3.3. Chemical Forms of Cadmium by Cd L_{III}-edge µ-XANES

The comparison of the cadmium L_{III}-edge XANES spectra of the model compounds shows that this technique enables a clear distinction between S and O/N ligands since O/N ligands induce a peak at about at 3539 eV (Figure 5), as shown by Pickering et al. [27]. Solution complexes, and Cd-pectin, Cd-cellulose and Cd-cell wall display poorly structured spectra, and some of them (eg., Cd-malate and Cd-citrate) are hardly distinguishable. On the contrary, mineral Cd references exhibit characteristic

spectral features. Spectra of the frozen samples are noisier than the freeze-dried ones due to the lower Cd concentration and stronger absorption of the Cd X-ray fluorescence by water. However, spectra are not significantly different, indicating that Cd speciation is not altered by the freeze-drying treatment. Spectra of trichome (strip) and root (vascular bundle) are clearly different, suggesting different types of ligands for Cd. For the trichome spectra, the peak at 3539 eV indicates oxygen and/or nitrogen ligands while the absence of this peak in the root spectrum indicates sulfur ligands. This result is in agreement with the high level of S detected by µ-XRF (Figure 4E).

One-component fits for the freeze-dried trichome spectrum indicated that Cd-pectin was the closest reference (*NSS* = 0.110 for 103% Cd-pectin, Figure 6A, Table 1), followed by Cd-cell wall (*NSS* = 0.157 for 96% Cd-cell wall, Figure 6A, Table 1), and Cd-cellulose (*NSS* = 0.257 for 95% Cd-cellulose, Figure 6A, Table 1). For comparison, fits with Cd-oxalate, Cd-phosphate, and Cd-malate gave *NSS* of 0.436, 0.816 (Figure 6A, Table 1) and 0.567 (Table 1), respectively. These results are consistent with the binding of Cd with components of the cell wall or cuticle of the trichome. Best two-component fits were obtained for a mixture of Cd-pectin and Cd bound to S-containing ligands namely Cd-cystein, CdS, and Cd-glutathione (Figure 6A, Table 1). However, the decrease of *NSS* (*I*) was moderate ($I \ll 20\%$, Table 1), which suggests that the addition of a second component was not justified. Furthermore, the proportion of this second component is less than 10%, *i.e.*, within the precision of the method. For the frozen hydrated trichome, best spectral matches were also obtained with 103% Cd-pectin (*NSS* = 0.410, Figure 6B, Table 1), 97% Cd-cell wall (*NSS* = 0.436, Figure 6B, Table 1), and Cd-cellulose (*NSS* = 0.552, Figure 6B, Table 1). Cd-oxalate and Cd-malate gave poor spectral agreements (*NSS* = 0.573 and 0.638, Figure 6B, Table 1, fit not shown for Cd-

malate). Although Cd-phosphate provided the lowest *NSS* value (0.353, Figure 6B), the fit was visually weaker. Particularly, this reference spectrum has a shoulder between 3548 and 3556 eV, which is absent in the trichome spectrum. Thus, this fit was not retained. Adding a second component moderately improved the simulation (I < 20%, Table 1) and best fits were obtained with a second component containing sulfhydryl groups. The proportion of this second component accounted for more than 25%, so in this case, the two-component simulation was retained. The XANES spectrum collected a few micrometers away from the trichome strip exhibited a slightly less pronounced peak, suggesting an enhanced contribution of S ligands in the rest of the trichomes (not shown).

The root spectra were best reproduced by Cd-cysteine or Cd-glutathione, and the latter reference provided a slightly better fit (*NSS* = 0.080 with 102% Cd-glutathione, and *NSS* = 0.291 with 110% Cd-cysteine for the freeze-dried root, Figure 6C, and *NSS* = 0.137 with 98% Cd glutathione, and *NSS* = 0.143with 106% Cd-cysteine for the frozen sample, Figures 6D, Table 1). Note that CdS yielded poorer match (Figures 6C, Table 1). Based on the I parameter, the addition of a second component significantly improved the fit, and best results were obtained for a combination of Cd-glutathione and Cd associated to cell wall constituents (Figures 6C and D Table 1). However, the presence of this second component should be considered with caution since its proportion (~10%) is within the precision of the method.

4. Discussion

4.1. Plant Growth and Cadmium Concentrations

After 4 days of exposition to 200 µM Cd, root growth was inhibited. Similar observation was found by Suzuki [28] with 1-week-old *A. thaliana* seedlings exposed to

200 µM Cd during 1 week. Wojcik et al. [29] reported a 50% reduction in root elongation after 4 days of exposure to 100 µM Cd in hydroponics, where ion diffusion and availability is increased compared to agar medium. Measured Cd concentrations were also consistent with other work reporting ~1000 mg Cd $.kg^{-1}$ in roots and ~500 mg Cd $.kg^{-1}$ in shoots after 7 days at 100 µM Cd [29]. Higher metal concentrations in roots than in leaves are typical of non accumulating plants.

4.2. Sequestration of Cadmium

Sequestration of various metals in trichomes has been observed in numerous plants, including hyperaccumulating species - zinc and cadmium in *Arabidopsis halleri* [30], nickel in *Alyssum murale* [31]- and non-hyperaccumulating species - manganese in *Helianthus annuus* [32], Cd in *Brassica juncea* [7]. In the hyperaccumulating plants *A. halleri*, although trichomes present the highest metal concentrations, mesophyll cells are the major storage site for metal in leaves [6,35]. Here, we found that the leaf tissues *i.e.* epidermis and mesophyll contained only traces of cadmium, and trichomes were likely the major Cd storage compartment for cadmium. The sequestration of Cd in these trichomes might be a way to protect the metabolically active cells from metal toxicity. High content of Cd in the trunk of the trichomes of *A. thaliana* was previously observed by Ager et al. [12] using micro-PIXE. The present study provides new insights on the chemical form of Cd in trichomes. We found that about 75% of Cd was bound to O/N atoms, likely belonging to cell wall or cuticle of the trichome. Cell walls are mainly composed of polysaccharides including cellulose, hemicellulose and pectin, providing hydroxyl functional groups (cellulose and hemicellulose), and hydroxyl plus carboxyl functional groups (pectin). Cd L_{III}-edge XANES spectroscopy is not sensitive enough to

distinguish between these possible binding molecules, but we suggest that Cd could be associated to pectin, due to the high affinity of this biopolymer for cations [33,34]. Furthermore, we observed a thickening of the trunk of trichomes in the region of the strip (arrow in Figure 3A). This might correspond to some enrichment in pectin, known as a swelling compound. Due to the small thickness of the bumps, it was not possible to isolate their XANES spectrum from the underlying part of the trichome. The Cd enrichment in the bumps and in the tips of the trichomes might result from evapotranspiration. A small proportion (about 25%) of Cd was bound to S-containing ligands. This second species, evidenced on the frozen hydrated sample, was below the detection limit for the freeze-dried sample. Thus, freeze-drying may slightly modify Cd speciation. Also, the difference may arise from the fact that the sampling depth differs between the two sample conditionings. Moreover, the level of noise for the hydrated sample is relatively high, so this difference should be considered with caution. The possible presence of Cd-S complexes would be consistent with the high levels of glutathione observed in *A. thaliana* trichomes [13,14] and cells [9] under Cd exposure. At the opposite, XANES results ruled out the sequestration of cadmium by oxalate, often reported as an immobilizing ligand for metals in plants.

In roots, Cd was distributed in the vascular bundles. Investigations were performed on whole roots and not on thin sections, and consequently we were unable to differentiate xylem and phloem vessels. Cd was unambiguously bound to sulfur ligands, and coordinated to the thiol groups of cysteine, which may belong to glutathione, or to larger molecules such as metallothioneins and phytochelatins (not tested). This is consistent with the high affinity of thiols for Cd, and with the role of these cysteine-containing compounds in Cd detoxification [36,37]. The sequestration of cadmium by

phytochelatins was clearly evidenced in roots in Indian mustard [38]. We identified S ligands in leaf veins but the XANES spectrum was very noisy due to the low concentration of Cd (data not shown). This suggests that Cd could be transported as stable sulfur complex, as observed in *Thlaspi caerulescens* [39].

5. Conclusions

This study illustrates the sensitivity of Cd L_{III}-edge XANES spectroscopy to discriminate different Cd local structures, particularly O/N ligands from S ligands. However, this technique is not sensitive enough to distinguish complexes with similar Cd environments, e.g., Cd-malate and Cd-citrate, or Cd-cystein and Cd-glutathione. To our knowledge, Cd L_{III}-edge XANES spectroscopy has been used in the past by Pickering et al. [27] on cadmium phytochelatins and model compounds, and it is the first time it is applied to plant samples. The possibility to combine µ-XRF for the localization and µ-XANES for the speciation with sub-micron resolution provides a precious tool for the study of Cd storage and trafficking in biological samples at the cellular scale. Similar results were obtained on frozen hydrated and freeze-dried plant samples concerning the localization and the speciation of Cd. This suggests that the freeze-drying treatment did not induce a redistribution of Cd in the plant cells. However, this may not be the case for other cations, especially those having a lower affinity for organic ligands. Cadmium is a highly toxic element, and Cd concentrations found in the environment are very low. In this study, plant exposure to cadmium was relatively high in order to ensure a reasonable Cd content (550 $mg.kg^{-1}$ dry weight in leaves, i.e., about 5 $mg.kg^{-1}$ fresh weight). Working on more realistic samples would require the lowering of the detection limit of the spectrometer. Increasing the photons

flux would enhance radiation damages on the samples, so a better strategy would be to improve the fluorescence detection system.

Acknowledgments

We are grateful to the European Synchrotron Radiation Facility (Grenoble, France) for the provision of beam time, and ID-21 staff and Nicolas Geoffroy from the LGIT for their technical support during data collection. We acknowledge Benoit Jaillard from UMR Rhizosphere & Symbiose at ENSAM, Montpellier, France, for providing isolated root cell walls. The authors also thank the three anonymous reviewers for scientific advices.

References

[1] M.J. McLaughlin, B.R. Singh, Cadmium in Soils and Plants, in: M.J. McLaughlin, B.R. Singh (Eds.), Cadmium in Soils and Plants, Kluwer Academic Publishers, Dordrecht, 1999, pp. 1-9.
[2] W.E. Rauser, Phytochelatins and related peptides, Plant Physiol. 109 (1995) 1141-1149.
[3] M. Wojcik, J. Vangronsveld, D.H. J, A. Tukiendorf, Cadmium tolerance in Thlaspi caerulescens - II. Localization of cadmium in *Thlaspi caerulescens*, Environ. Exp. Bot. 53 (2) (2005) 163-171.
[4] J.F. Ma, D. Ueno, F.J. Zhao, S.P. McGrath, Subcellular localisation of Cd and Zn in the leaves of a Cd-hyperaccumulating ecotype of *Thlaspi caerulescens*, Planta 220 (5) (2005) 731-736.
[5] M.D. Vazquez, J. Barcelo, C. Poschenrieder, J. Madico, P. Hatton, A.J.M. Baker, G.H. Cope, Localization of zinc and cadmium in *Thlaspi caerulescens* (brassicaceae), a metallophyte that can hyperaccumulate both metals, J. Plant Physiol. 140 (1992) 350-355.
[6] H. Kupper, E. Lombi, F.J. Zhao, S.P. McGrath, Cellular compartmentation of cadmium and zinc in relation to other elements in the hyperaccumulator *Arabidopsis halleri*, Planta 212 (2000) 75-84.
[7] D.E. Salt, R.C. Prince, I.J. Pickering, I. Raskin, Mechanisms of cadmium mobility and accumulation in Indian mustard, Plant Physiol. 109 (1995) 1427-1433.
[8] Y. Choi, E. Harada, M. Wada, H. Tsuboi, Y. Morita, T. Kusano, S. H, Detoxification of cadmium in tobacco plants: formation and active excretion of crystals containing cadmium and calcium through trichomes, Planta 213(1) (2001) 45-50.

[9] J.E. Sarry, L. Kuhn, C. Ducruix, A. Lafaye, C. Junot, V. Hugouvieux, A. Jourdain, O. Bastien, J.B. Fievet, D. Vailhen, B. Amekraz, C. Moulin, E. Ezan, J. Garin, J. Bourguignon, The early responses of *Arabidopsis thaliana* cells to cadmium exposure explored by protein and metabolite profiling analyses, Proteomics 6 (7) (2006) 2180-2198.
[10] U. Kramer, Phytoremediation to phytochelatin-plant trace metal homeostasis, New Phytol. 158 (2003) 1-9.
[11] B. Elbaz, N. Shoshani Knaani, O. David Assael, T. Mizrachy Dagri, K. Mizrahi, H. Saul, E. Brook, I. Berezin, O. Shaul, High expression in leaves of the zinc hyperaccumulator *Arabidopsis halleri* of AhMHX, a homolog of an *Arabidopsis thaliana* vacuolar metal proton exchanger, Plant Cell Environ. 29 (6) (2006) 1179-1190.
[12] F.J. Ager, M.D. Ynsa, J.R. Dominguez Solis, M.C. Lopez Martin, C. Gotor, L.C. Romero, Nuclear micro-probe analysis of *Arabidopsis thaliana* leaves, Nucl. Instrum. Meth. B 210 (2003) 401-406.
[13] G. Gutierrez Alcala, C. Gotor, A.J. Meyer, M. Fricker, J.M. Vega, L.C. Romero, Glutathione biosynthesis in Arabidopsis trichome cells, P. Natl. Acad. Sci. USA. 97 (20) (2000) 11108-11113.
[14] J.R. Dominguez Solis, M.C. Lopez Martin, F.J. Ager, M.D. Ynsa, L.C. Romero, C. Gotor, Increased cysteine availability is essential for cadmium tolerance and accumulation in *Arabidopsis thaliana*, Plant Biotechnol. J. 2 (6) (2004) 469-476.
[15] A. Manceau, M.A. Marcus, N. Tamura, Quantitative speciation of heavy metals in soils and sediments by synchrotron X-ray techniques, in: P. Fenter, M. Rivers, N. Sturchio, S. Sutton (Eds.), Applications of Synchrotron Radiation in Low-Temperature Geochemistry and Environmental Science, Reviews in Mineralogy and Geochemistry, Mineralogical Society of America, Washington, DC., 2002, pp. 341-428.
[16] K.G. Scheckel, E. Lombi, S.A. Rock, N.J. McLaughlin, In vivo synchrotron study of thallium speciation and compartmentation in *lberis intermedia*, Environ. Sci. Technol. 38 (19) (2004) 5095-5100.
[17] D. Van Hoewyk, G.F. Garifullina, A.R. Ackley, S.E. Abdel Ghany, M.A. Marcus, S. Fakra, K. Ishiyama, E. Inoue, M. Pilon, H. Takahashi, E.A.H. Pilon Smits, Overexpression of AtCpNifS enhances selenium tolerance and accumulation in Arabidopsis, Plant Physiol. 139 (3) (2005) 1518-1528.
[18] T.G. Sors, D.R. Ellis, G.N. Na, B. Lahner, S. Lee, T. Leustek, I.J. Pickering, D.E. Salt, Analysis of sulfur and selenium assimilation in Astragalus plants with varying capacities to accumulate selenium, Plant J. 42 (6) (2005) 785-797.
[19] T. Punshon, A. Lanzirotti, S. Harper, P.M. Bertsch, J. Burger, Distribution and speciation of metals in annual rings of black willow, J. Environ. Quality 34 (4) (2005) 1165-1173.
[20] J.A. Howe, R.H. Loeppert, V.J. Derose, D.B. Hunter, P.M. Bertsch, Localization and speciation of chromium in subterranean clover using XRF, XANES, and EPR spectroscopy, Environ. Sci. Technol. 37 (18) (2003) 4091-4097.
[21] K.M. Kemner, S.D. Kelly, B. Lai, J. Maser, O.L. EJ, D. Sholto Douglas, Z.H. Cai, M.A. Schneegurt, C.F. Kulpa, K.H. Nealson, Elemental and redox analysis of single bacterial cells by X-ray microbeam analysis, Science 306 (5296) (2004) 686-687.
[22] P.M. Oger, I. Daniel, B. Cournoyer, A. Simionovici, In situ micro X-ray absorption near edge structure study of microbiologically reduced selenite (SeO32-), Spectrochim. Acta B 59 (10-11) (2004) 1681-1686.
[23] J. Chwiej, M. Szczerbowska Boruchowska, M. Lankosz, S. Wojcik, G. Falkenberg,

Z. Stegowski, Z. Setkowicz, Preparation of tissue samples for X-ray fluorescence microscopy, Spectrochim. Acta B 60 (12) (2005) 1531-1537.
[24] D.L. Parkhurst, C.A. Appelo, User's guide to PhreeqC (version 2), A computer program for speciation, batch-reaction, one-dimensional transport, and inverse geochemical calculations, U.S. Geological Survey Water Resource Inv. (1999) 99-4259.
[25] J. Susini, M. Salome, B. Fayard, R. Ortega, B. Kaulich, The scanning X-ray microprobe at the ESRF "x-ray microscopy" beamline, Surf. Rev. Lett. 9 (1) (2002) 203-211.
[26] T. Punshon, B.P. Jackson, A. Lanzirotti, W.A. Hopkins, P.M. Bertsch, J. Burger, Application of synchrotron x-ray microbeam spectroscopy to the determination of metal distribution and speciation in biological tissues, Spectroscopy Lett. 38 (3) (2005) 343-363.
[27] I.J. Pickering, R.C. Prince, G.N. George, W.E. Rauser, W.A. Wickramasinghe, A.A. Watson, C.T. Dameron, I.G. Dance, D.P. Fairlie, D.E. Salt, X-ray absorption spectroscopy of cadmium phytochelatin and model systems, Biochim. Biophys. Acta 1429 (2) (1999) 351-364.
[28] N. Suzuki, Alleviation by calcium of cadmium-induced root growth inhibition in Arabidopsis seedlings, Plant Biotechnol. 22 (2005) 19-25.
[29] M. Wojcik, A. Tukiendorf, Phytochelatin synthesis and cadmium localization in wild type of *Arabidopsis thaliana*, Plant Growth Regul. 44 (1) (2004) 71-80.
[30] F. Zhao, E. Lombi, T. Breedon, S. McGrath, Zinc hyperaccumulation and cellular distribution in *Arabidopsis halleri*, Plant Cell Environ. 23 (2000) 507-514.
[31] C.L. Broadhurst, R.L. Chaney, J.S. Angle, T.K. Maugel, E.F. Erbe, C.A. Murphy, Simultaneous hyperaccumulation of nickel, manganese, and calcium in Alyssum leaf trichomes, Environ. Sci. Technol. 38 (21) (2004) 5797-5802.
[32] F.P.C. Blamey, D.C. Joyce, D.G. Edwards, C.J. Asher, Role of trichomes in sunflower tolerance to manganese toxicity, Plant Soil 91 (1986) 171-180.
[33] N. Cohen Shoel, D. Ilzycer, I. Gilath, E. Tel Or, The involvement of pectin in Sr^{2+} biosorption by Azolla, Water Air Soil Poll. 135 (1-4) (2002) 195-205.
[34] J.B. Wehr, N.W. Menzies, F.P.C. Blamey, Inhibition of cell-wall autolysis and pectin degradation by cations, Plant Physiol. Bioch. 42 (6) (2004) 485-492.
[35] G. Sarret, P. Saumitou-Laprade, V. Bert, O. Proux, J.L. Hazemann, A. Traverse, M.A.M. Marcus, A. Manceau, Forms of zinc accumulated in the hyperaccumulator *Arabidopsis halleri*., Plant Physiol. 130 (2002) 1815-1826.
[36] R. Howden, P.B. Goldsborough, C.R. Andersen, C.S. Cobbett, Cadmium-sensitive, cad1 mutants of *Arabidopsis thalina* are phytochelatin deficient, Plant Physiol. 107 (1995) 1059-1066.
[37] C.S. Cobbett, Phytochelatins and their roles in heavy metal detoxification, Plant Physiol. 123 (3) (2000) 825-832.
[38] D.E. Salt, I.J. Pickering, R.C. Prince, D. Gleba, S. Dushenkov, R.D. Smith, I. Raskin, Metal accumulation by aquacultured seedlings of Indian mustard, Environ. Sci. Technol. 31 (1997) 1636-1644.
[39] H. Küpper, A. Mijovilovich, W. Meyer-Klaucke, P.M.H. Kroneck, Tissue-and Age-dependent differences in the complexation of cadmium and zinc in the cadmium/zinc hyperaccumulator *Thlaspi caerulescens* (Ganges ecotype) revealed by X-ray absorption spectroscopy., Plant Physiol. 134 (2004) 748-757.

Tables

Table 1: One- and two-component fits (in % mole fraction) of Cd L_{III}-edge µ-XANES spectra

Sample	One-component fit		Two-component fit		
	% compound	***NSS*[a] *(%)***	**% compound**	***NSS*[a] *(%)***	***I*[b] (%)**
Freeze-dried Trichome	103 Cd-pectin	0.110	91 Cd-pectin + 9 Cd-cysteine	0.092	16.4
	96 Cd-cell wall	0.157	94 Cd-pectin + 6 CdS	0.095	13.6
	95 Cd-cellulose	0.257	94 Cd-pectin + 6 Cd-glutathione	0.101	8.2
	94 Cd-oxalate	0.436			
	93 Cd-malate	0.567			
	92 Cd-phosphate	0.816			
Frozen Trichome	93 Cd-phosphate	0.353	74 Cd-pectin + 26 Cd-glutathione	0.287	18.7
	103 Cd-pectin	0.410	64 Cd-pectin + 40 Cd-cysteine	0.314	11.0
	97 Cd-cell wall	0.436	78 Cd-pectin + 25 CdS	0.332	5.9
	95 Cd-cellulose	0.552			
	94 Cd-oxalate	0.573			
	93 Cd-malate	0.638			
Freeze-dried Root	102 Cd-glutathione	0.080	91 Cd-glutathione + 12 Cd-cellulose	0.051	36.2
	110 Cd-cysteine	0.291	89 Cd-glutathione + 14 Cd-cell wall	0.054	32.5
	110 CdS	0.426	91 Cd-glutathione + 12 Cd-pectin	0.056	30.0
Frozen Root	98 Cd-glutathione	0.137	90 Cd-glutathione + 9 Cd-pectin	0.102	25.5
	106 Cd-cysteine	0.143	89 Cd-glutathione + 10 Cd-cell wall	0.104	24.1
	105 CdS	0.262	91 Cd-glutathione + 7 Cd-malate	0.126	8.0

[a] Residual between fit and experimental data : $NSS = \Sigma(\text{Xanes}_{\text{experimental}} - \text{Xanes}_{\text{fit}})^2 / \Sigma(\text{Xanes}_{\text{experimental}})^2 \times 100$, in the 3530-3580 eV range.

[b] Improvement of the fit : $I = 100 - (NSS_{\text{two-component}} * 100 / NSS_{\text{best one-fit component}})$.

Captions

Figure 1 Influence of cadmium on growth in *Arabidopsis thaliana* plants (A, B, C), and trichomes covering the surface of leaves (D). A: 12-day old plants before their transfer in the contaminated medium. B: Control plants grown in a non contaminated medium for 16 days, C: 16-day old plants grown in medium contaminated with 200 µM Cd during 4 days. For A, B, C: scale bar = 2 cm. For D: scale bar = 2 mm.

Figure 2 Trichome observed on a freeze-dried leaf by SEM-EDX in secondary electron (SE) (A) and backscattering electron (BSE) mode (B) (scale bar = 100 µm), and elemental profile analyses from point a to point b obtained by EDX (C-F, step = 2 µm).

Figure 3 Detail of the trichome obtained by SEM in secondary electron mode (SE) (A, scale bar = 10 µm), X-ray fluorescence spectra collected on a bump and in the matrix a few microns away from the bump (B), and elemental distributions in negative contrast obtained by EDX (C, scale bar = 2 µm). Arrow in A indicates a thickening of the trichome trunk.

Figure 4 False-color µ-XRF elemental maps recorded on a leaf containing trichomes (A, scale bar = 70 µm) and on a root (B, scale bar = 25 µm), and X-ray fluorescence spectra collected on the trichome strip (C, point 1 in Figure 4A), on the leaf tissue (D, point 2 in Figure 4A), on the central vascular bundle on the root (E, point 1 in Figure 4B), and on the border of the root (F, point 2 in Figure 4B). For the maps, step-size =1 µm, dwell time = 500 ms/pixel at 3550 eV, and 100 and 250 ms/pixel at 4100 eV for leaf and root, respectively.

Figure 5 Cadmium L_{III}-edge XANES spectra of *Arabidopsis thaliana* trichome and root examined as freeze-dried and frozen samples, and reference compounds: A, $CdCO_3$; B, CdO; C, $Cd_5H_2(PO_4)_4.4H_2O$; D, $CdSO_4$; E, Cd^{2+}_{aq}; F, $CdCl_2$; G, Cd-oxalate; H, Cd-acetate; I, Cd-histidine$_{aq}$; J, Cd-citrate$_{aq}$; K, Cd-malate$_{aq}$; L, Cd-Cell Wall; M, Cd-cellulose; N, Cd-pectin; O, Cd-glutathione$_{aq}$; P, Cd-cysteine$_{aq}$; and Q, CdS. $CdCO_3$, CdO, $Cd_5H_2(PO_4)_4.4H_2O$, $CdSO_4$, $CdCl_2$, Cd-oxalate, Cd-acetate, Cd-Cell Wall, and CdS were solid-powdered samples.

Figure 6 One- and two-component fits of Cd L_{III}-edge XANES spectra for *Arabidopsis thaliana* freeze-dried trichome (A), frozen trichome (B), freeze-dried root (C), and frozen root (D). The quality of the fit is evaluated by the normalized sum-squares residuals, *NSS* $= \Sigma_i (\text{Xanes}_{\text{experimental}} - \text{Xanes}_{\text{fit}})^2 / \Sigma_i (\text{Xanes}_{\text{experimental}})^2 \times 100$, indicated in parentheses.

Figure(s)

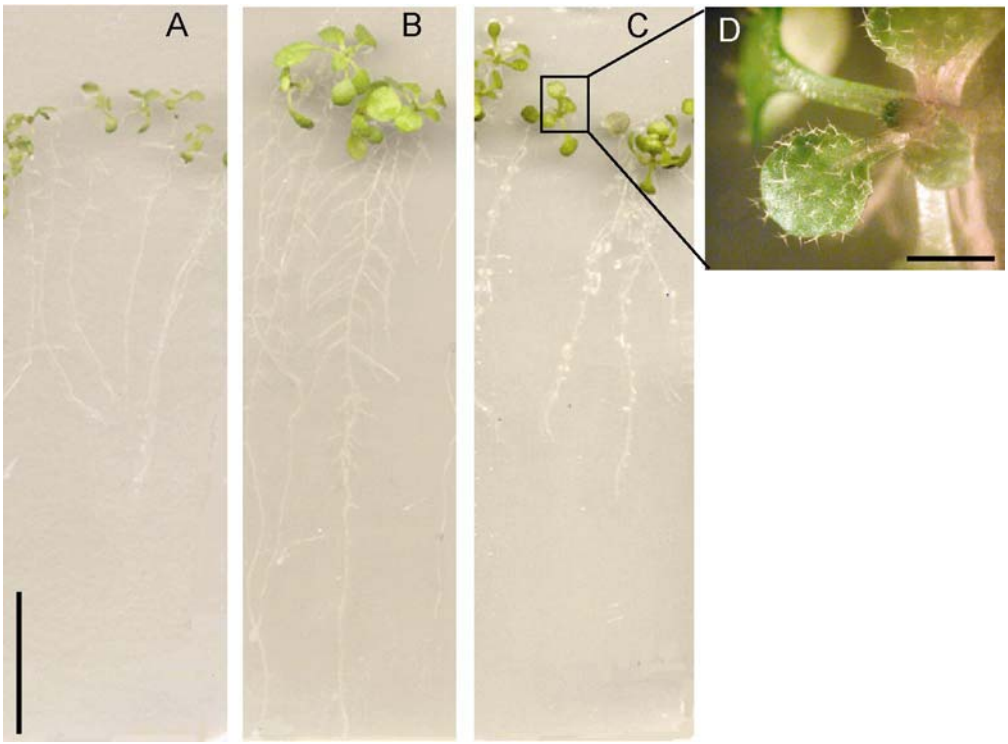

Fig.1

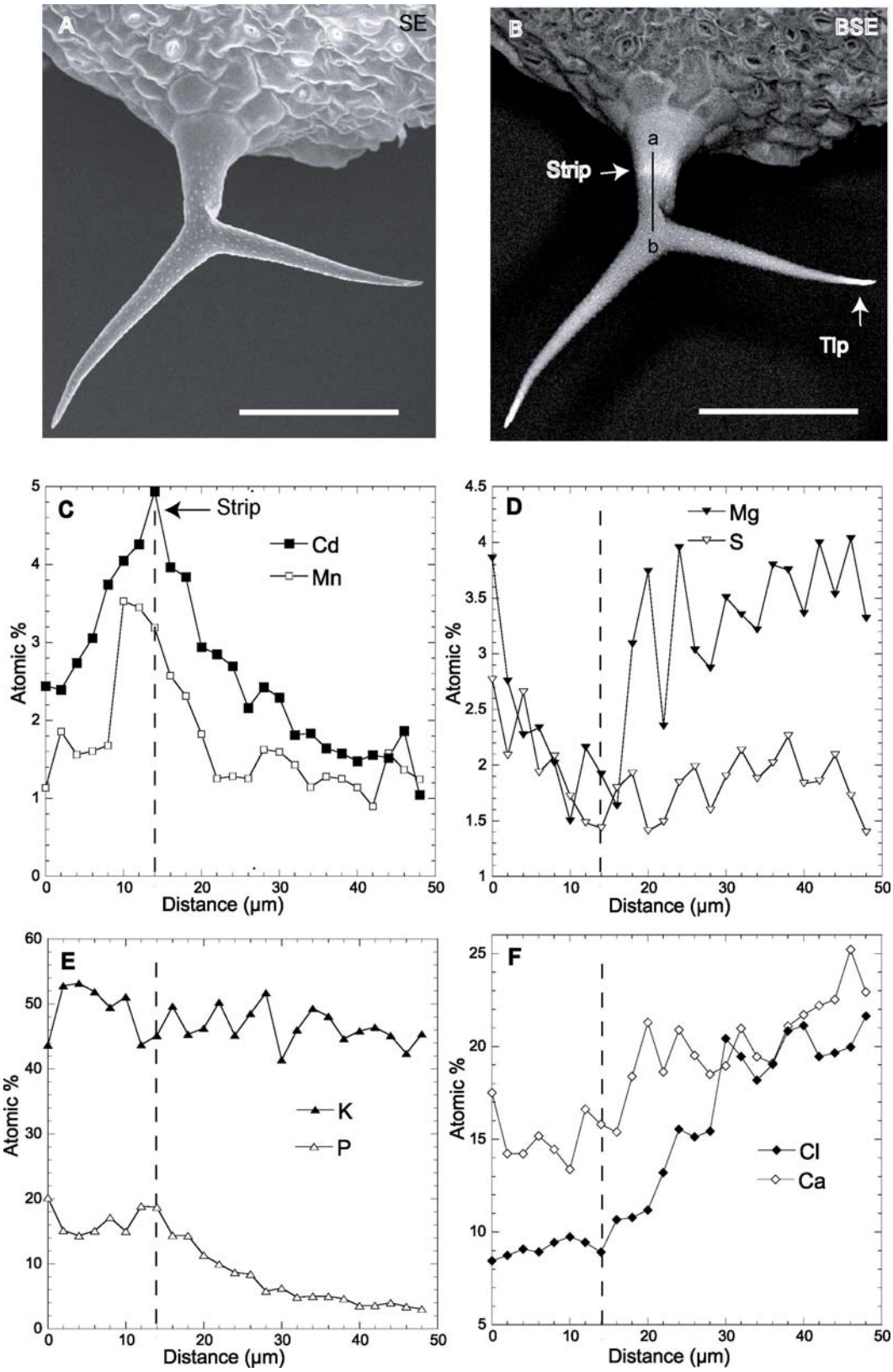
A
SE
B
BSE
a
Strip
b
Tip
C
Strip
Cd
Mn
Atomic %
Distance (μm)
D
Mg
S
Atomic %
Distance (μm)
E
K
P
Atomic %
Distance (μm)
F
Cl
Ca
Atomic %
Distance (μm)

Fig. 2

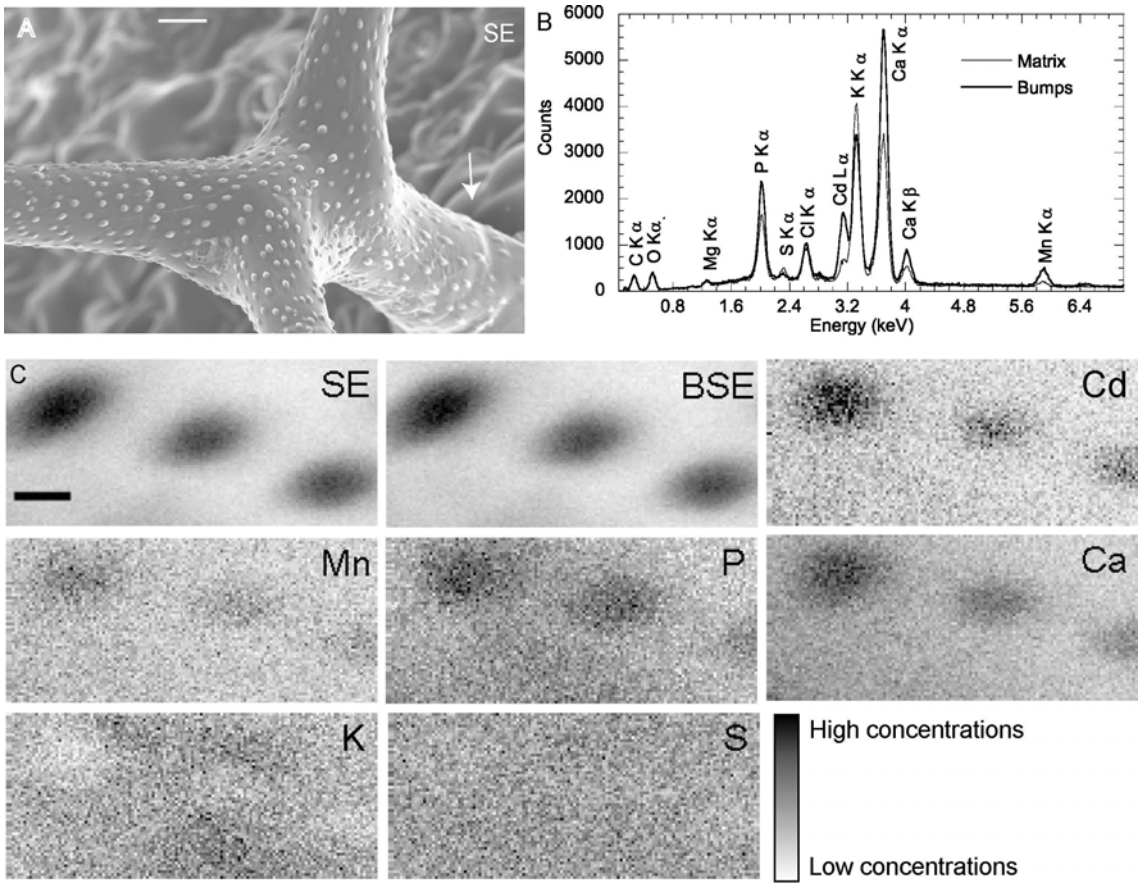
A
SE
B
Counts
Energy (keV)
Matrix
Bumps
C K α
O Kα.
Mg Kα
P Kα
S Kα
Cl K α
Cd L α
K K α
Ca K α
Ca K β
Mn K α
C
SE
BSE
Cd
Mn
P
Ca
K
S
High concentrations
Low concentrations

Fig. 3

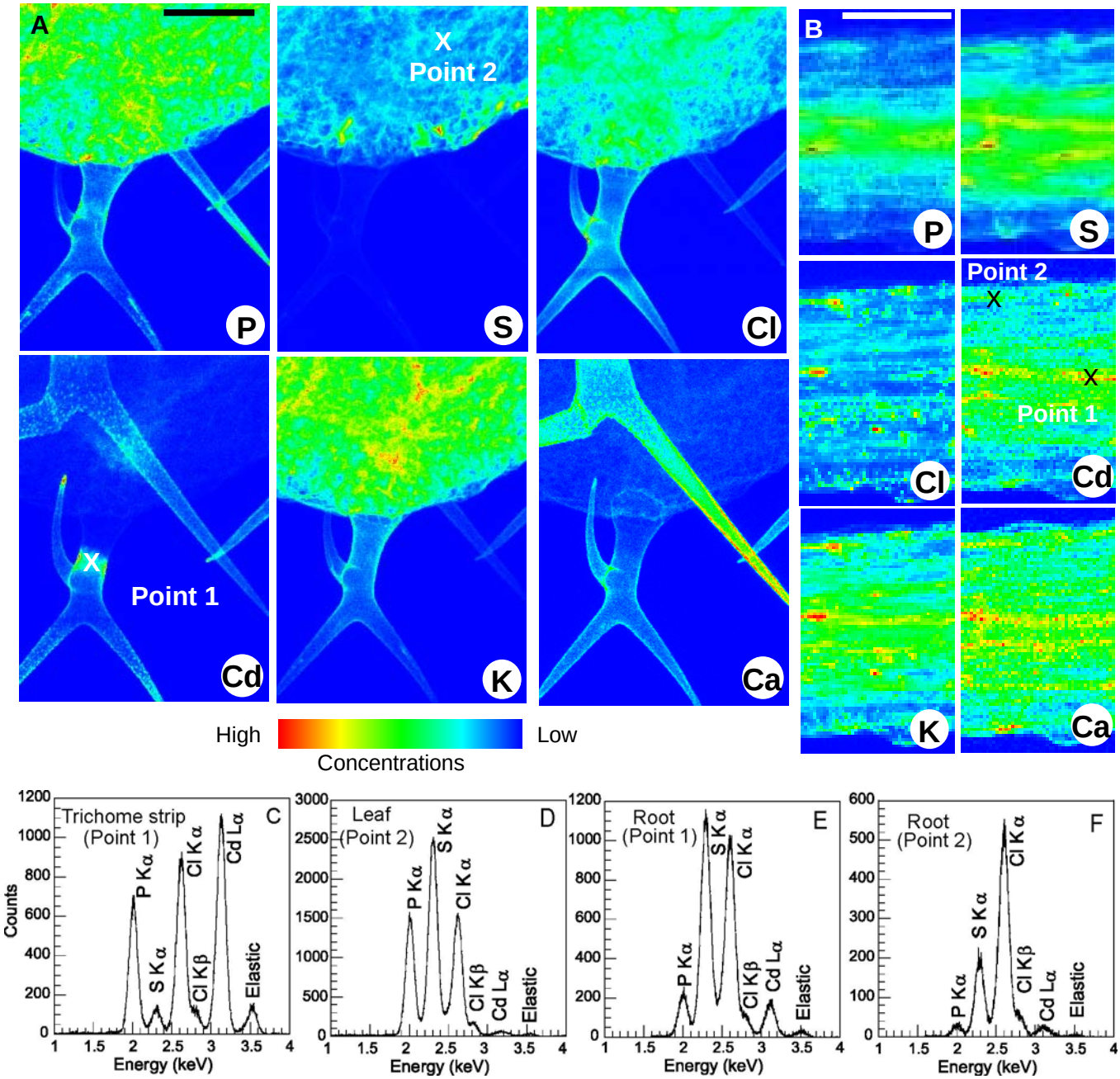
A
X
Point 2
P
S
Cl
X
Point 1
Cd
K
Ca
High
Low
Concentrations
B
P
S
Point 2
X
X
Point 1
Cl
Cd
K
Ca
Trichome strip
(Point 1)
C
Leaf
(Point 2)
D
Root
(Point 1)
E
Root
(Point 2)
F
P Kα
S Kα
Cl Kα
Cl Kβ
Cd Lα
Elastic
Counts
Energy (keV)

Fig. 4

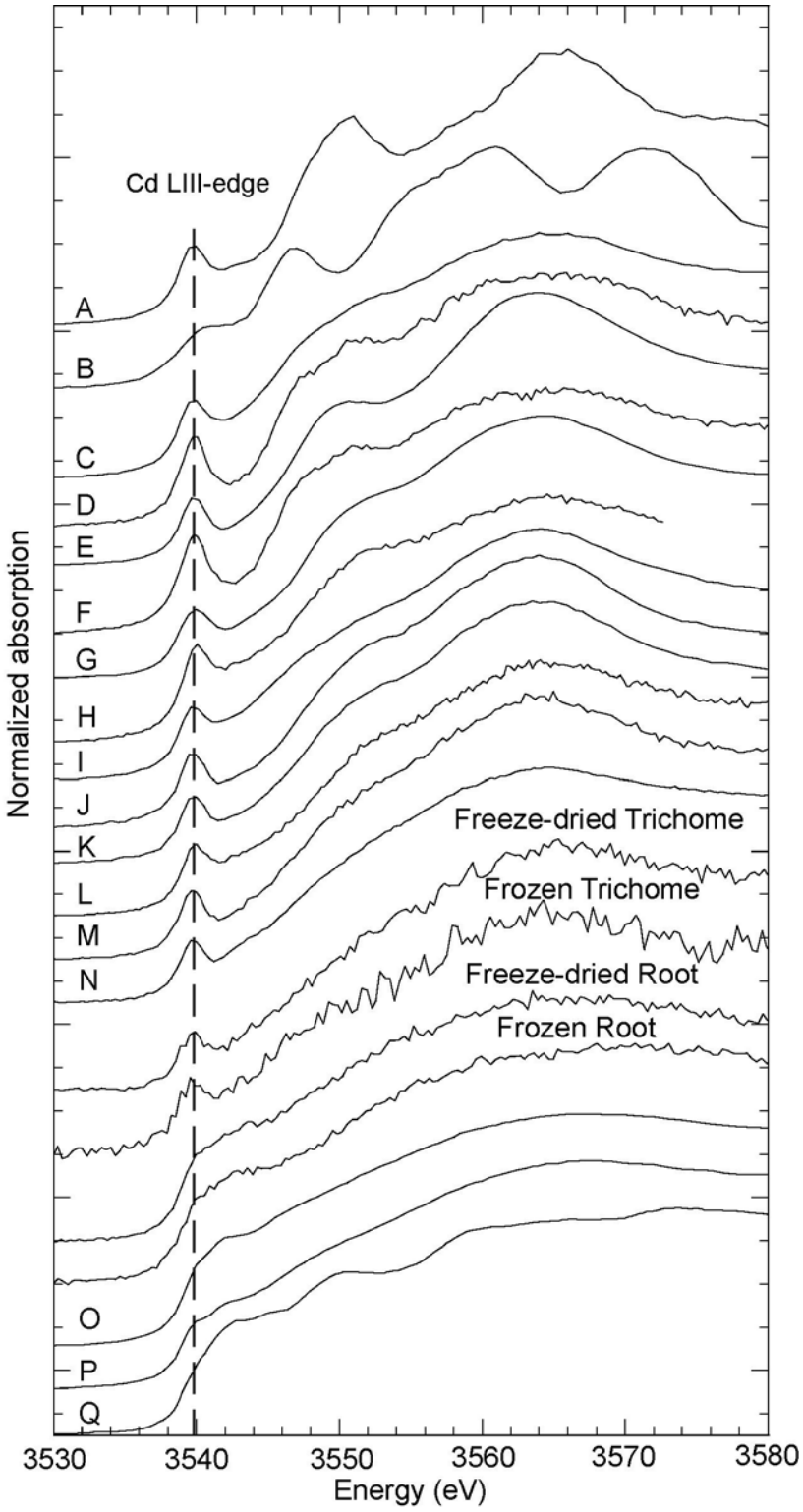
Cd LIII-edge
A
B
C
D
E
F
G
H
I
J
K
L
M
N
O
P
Q
Freeze-dried Trichome
Frozen Trichome
Freeze-dried Root
Frozen Root
Normalized absorption
3530
3540
3550
3560
3570
3580
Energy (eV)

Fig. 5

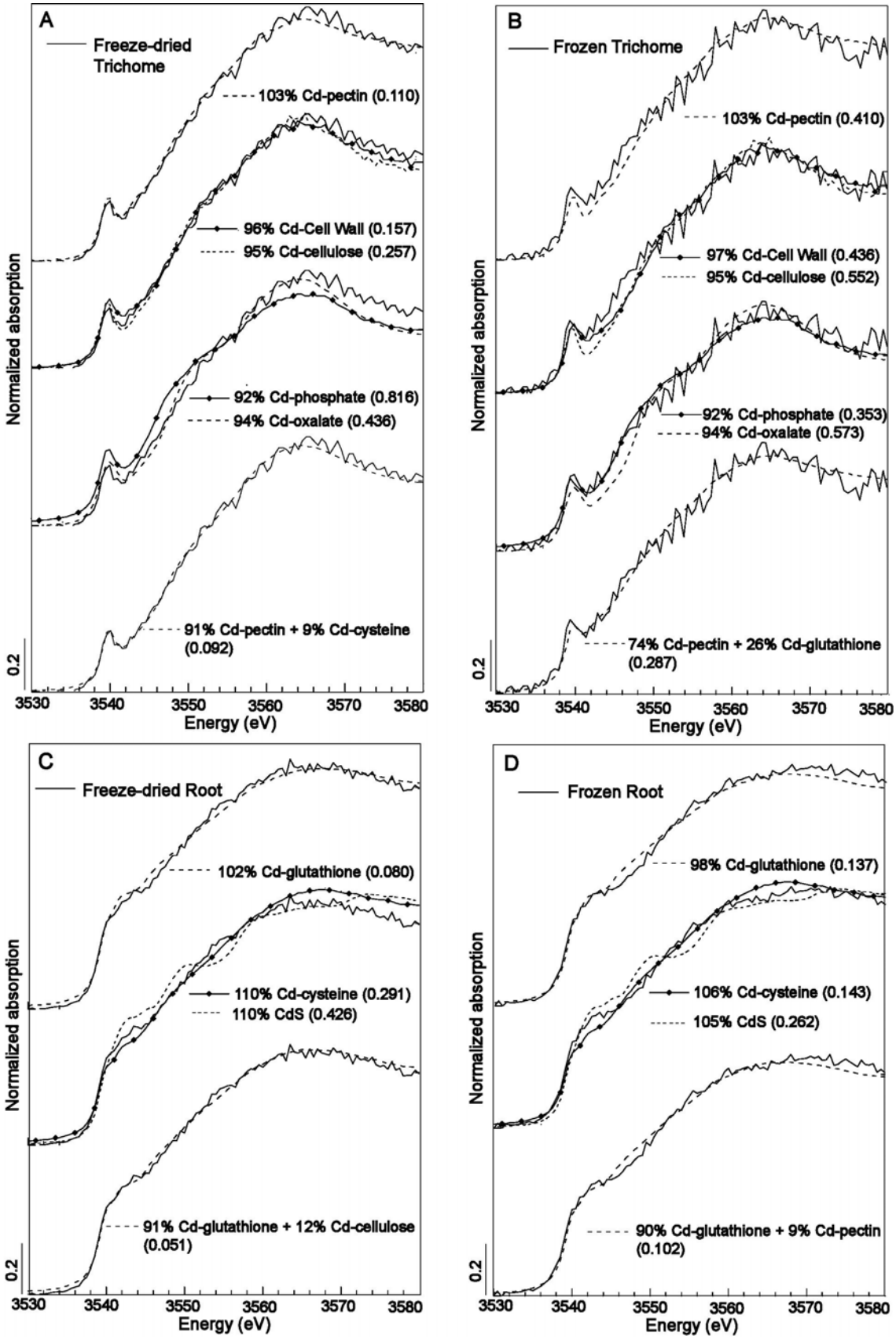
A
Freeze-dried Trichome
103% Cd-pectin (0.110)
96% Cd-Cell Wall (0.157)
95% Cd-cellulose (0.257)
92% Cd-phosphate (0.816)
94% Cd-oxalate (0.436)
91% Cd-pectin + 9% Cd-cysteine (0.092)
Normalized absorption
0.2
3530 3540 3550 3560 3570 3580
Energy (eV)
B
Frozen Trichome
103% Cd-pectin (0.410)
97% Cd-Cell Wall (0.436)
95% Cd-cellulose (0.552)
92% Cd-phosphate (0.353)
94% Cd-oxalate (0.573)
74% Cd-pectin + 26% Cd-glutathione (0.287)
Normalized absorption
0.2
3530 3540 3550 3560 3570 3580
Energy (eV)
C
Freeze-dried Root
102% Cd-glutathione (0.080)
110% Cd-cysteine (0.291)
110% CdS (0.426)
91% Cd-glutathione + 12% Cd-cellulose (0.051)
Normalized absorption
0.2
3530 3540 3550 3560 3570 3580
Energy (eV)
D
Frozen Root
98% Cd-glutathione (0.137)
106% Cd-cysteine (0.143)
105% CdS (0.262)
90% Cd-glutathione + 9% Cd-pectin (0.102)
Normalized absorption
0.2
3530 3540 3550 3560 3570 3580
Energy (eV)

Fig.6

Table(s)

Tables

Table 1: One- and two-component fits (in % mole fraction) of Cd L_{III}-edge µ-XANES spectra

Sample	One-component fit		Two-component fit		
	% compound	***NSS*[a] *(%)***	**% compound**	***NSS*[a] *(%)***	***I*[b] (%)**
Freeze-dried Trichome	103 Cd-pectin	0.110	91 Cd-pectin + 9 Cd-cysteine	0.092	16.4
	96 Cd-cell wall	0.157	94 Cd-pectin + 6 CdS	0.095	13.6
	95 Cd-cellulose	0.257	94 Cd-pectin + 6 Cd-glutathione	0.101	8.2
	94 Cd-oxalate	0.436			
	93 Cd-malate	0.567			
	92 Cd-phosphate	0.816			
Frozen Trichome	93 Cd-phosphate	0.353	74 Cd-pectin + 26 Cd-glutathione	0.287	18.7
	103 Cd-pectin	0.410	64 Cd-pectin + 40 Cd-cysteine	0.314	11.0
	97 Cd-cell wall	0.436	78 Cd-pectin + 25 CdS	0.332	5.9
	95 Cd-cellulose	0.552			
	94 Cd-oxalate	0.573			
	93 Cd-malate	0.638			
Freeze-dried Root	102 Cd-glutathione	0.080	91 Cd-glutathione + 12 Cd-cellulose	0.051	36.2
	110 Cd-cysteine	0.291	89 Cd-glutathione + 14 Cd-cell wall	0.054	32.5
	110 CdS	0.426	91 Cd-glutathione + 12 Cd-pectin	0.056	30.0
Frozen Root	98 Cd-glutathione	0.137	90 Cd-glutathione + 9 Cd-pectin	0.102	25.5
	106 Cd-cysteine	0.143	89 Cd-glutathione + 10 Cd-cell wall	0.104	24.1
	105 CdS	0.262	91 Cd-glutathione + 7 Cd-malate	0.126	8.0

[a] Residual between fit and experimental data : $NSS = \Sigma(\text{Xanes}_{\text{experimental}} - \text{Xanes}_{\text{fit}})^2 / \Sigma(\text{Xanes}_{\text{experimental}})^2 \times 100$, in the 3530-3580 eV range.

[b] Improvement of the fit : $I = 100 - (NSS_{\text{two-component}} * 100 / NSS_{\text{best one-fit component}})$.